Int. J. Electrochem. Sci., 14 **(2019)** 4986 – 4994, doi: 10.20964/2019.06.33

International Journal of
ELECTROCHEMICAL
SCIENCE
www.electrochemsci.org

Short Communication

Study of the Electrical Conductivity of Al(III) Doped $Sr_{0.6}Na_{0.4}SiO_{3-\alpha}$

Ruijuan Shi, Ruifeng Du, Junlong Liu[*]*, Hongtao Wang*[*]

School of Chemical and Material Engineering, Fuyang Normal University; Anhui Provincial Key Laboratory for Degradation and Monitoring of Pollution of the Environment, Fuyang 236037, China
[*]E-mail: hwang@fync.edu.cn; jlliu@fync.edu.cn

Received: 1 March 2019 / *Accepted:* 2 April 2019 / *Published:* 10 May 2019

$Sr_{1-x}Na_xSiO_{3-0.5x}$ is receiving worldwide attention as the fast oxide ion conductor. $Sr_{0.6}Na_{0.4}Si_{0.9}Al_{0.1}O_{3-\alpha}$ and $Sr_{0.6}Na_{0.4}SiO_{3-\alpha}$ were successfully fabricated using a solid state synthesis method and characterized with X-ray diffractometer (XRD) and scanning electron microscopy (SEM). From the results of XRD and SEM, it was demonstrated that both samples consist of crystalline $SrSiO_3$ and amorphous $Na_2Si_2O_5$. The Al^{3+} ion doping in the $Sr_{1-x}Na_xSiO_{3-\alpha}$ system led to the decrement of the amorphous Na-rich phase, and extended the scope of the oxide ionic conduction, though it resulted in a negative effect on the conductivity.

Keywords: Strontium silicate; Electrolyte; Fuel cell; Conductivity

1. INTRODUCTION

Solid oxide fuel cells (SOFCs) have attracted worldwide attention in the past decades because they can efficiently convert chemical energy into electrical energy, and they do not give off any greenhouse gases or other pollutants when hydrogen is used as the fuel. In an SOFC, an electrolyte, a porous anode, and a porous cathode are required, and the electrolyte material determines its operating temperature range [1-8]. However, the major challenge for the current cells is the high temperature of operation (over 800 °C). To address this issue, numerous efforts have been made toward the fabrication of electrolytes with high conductivities at intermediate temperature (500-800 °C) [9-14].

Recently, there has been a widening interest in a new family of layered alkali doped strontium silicates ($Sr_{1-x}A_xMO_{3-\delta}$, A = Na or K, M = Si or Ge), which, as promising electrolytes for intermediate temperature solid oxide fuel cells (IT-SOFCs), were initially introduced by Singh et al. [15-16]. They have demonstrated that the fast oxide ion conductors $Sr_{1-x}Na_xSiO_{3-0.5x}$ ($0 \leq x \leq 0.45$) were much less

hygroscopic than $Sr_{1-x}K_xSiO_{3-0.5x}$ and provided $\sigma_o \geq 10^{-2}$ $S \cdot cm^{-1}$ for $x \geq 0.40$ at 525 °C [16]. Subsequently, Wei et al. reported that a $Sr_{3-3x}Na_{3x}Si_3O_{9-1.5x}$ (x = 0.45) based IT-SOFC shows a peak power density of 431 $mW \cdot cm^{-2}$ at 600 °C [17]. These studies suggested that the mobile oxygen vacancies introduced by substitution of K^+ or Na^+ for Sr^{2+} were responsible for the high ionic conductivity of the alkali doped strontium silicate [15-18].

However, it has been argued by Bayliss et al. and Evans et al. that the dominant charge carrier was not the oxygen ion, and these Na- or K-doped $SrSiO_3$ materials were mixtures of crystalline $SrSiO_3$ and amorphous $K_2Si_2O_5$ or $Na_2Si_2O_5$ components with degrading conductivities [19-20]. In addition, they found that the amorphous material plays a significant role in the high ionic conductivity and the electrical performance increased with increasing amorphous phase content [19-21]. Variable temperature ^{23}Na solid state NMR spectroscopy and spin-lattice relaxation (T_1) measurements demonstrated that the Na^+ ions in $Sr_{0.60}Na_{0.40}SiO_{2.80}$ are highly mobile and the mobility of Na^+ ions becomes fast as the temperature is increased [22]. The result was supported by Chien et al. with high-resolution solid-state ^{29}Si, ^{23}Na, and ^{17}O NMR investigation on $Sr_{1-x}Na_xSiO_{3-0.5x}$ [23]. All these results disclosed that the majority of Na^+ ions did not incorporate into the $SrSiO_3$ structure and Na^+ ions in an amorphous $Na_2Si_2O_5$ phase were dominant charge carriers in nominal $Sr_{1-x}Na_xSiO_{3-0.5x}$ materials [22-24].

Although the amorphous $Na_2Si_2O_5$ phase was confirmed to be responsible for the high conductivity of $Sr_{1-x}Na_xSiO_{3-0.5x}$ ion conductors, the research of Tealdi et al. and Jee et al. showed that the amorphous $Na_2Si_2O_5$ crystallized to an electrical insulator with increasing temperature which caused the degradation of conductivities [25-27]. And Xu et al. also found that the amorphous phase $K_2Si_2O_5$ in $Sr_{0.8}K_{0.2}SiO_{2.85}$ material was transformed into crystalline SiO_2 and K_2SiO_3 at 650 °C, leading to the degradation of the ionic conductivities [28]. Furthermore, Sood et al. reported the glass transition (762 °C), glass melting (815 °C) and enthalpy of fusion (12.5 $J \cdot g^{-1}$) of the amorphous phase in the $Sr_{1-x}Na_xSiO_{3-0.5x}$ system [29].

In this paper, we synthesized sodium strontium silicate fast ion conductor of nominal composition $Sr_{0.6}Na_{0.4}SiO_{3-\alpha}$ and Al-doped sodium strontium silicate of nominal composition $Sr_{0.6}Na_{0.4}Si_{0.9}Al_{0.1}O_{3-\alpha}$. Their structure and electrical properties were studied by X-Ray diffraction, scanning electron microscopy and impedance spectroscopy. The effect of Al^{3+} ions doping on the structural and electrical properties of the $Sr_{0.6}Na_{0.4}SiO_{3-\alpha}$ was confirmed. The electrical properties of the $Sr_{0.6}Na_{0.4}Si_{0.9}Al_{0.1}O_{3-\alpha}$ and $Sr_{0.6}Na_{0.4}SiO_{3-\alpha}$ as electrolytes for intermediate temperature solid oxide fuel cells were also studied and discussed.

2. EXPERIMENTAL

$Sr_{0.6}Na_{0.4}Si_{0.9}Al_{0.1}O_{3-\alpha}$ and $Sr_{0.6}Na_{0.4}SiO_{3-\alpha}$ samples (denoted as SNSA and SNS, respectively) were prepared via solid state synthesis method from $SrCO_3$, Na_2CO_3, SiO_2 and Al_2O_3 (Sinopharm Chemical Reagent Co. Ltd., AR). The stoichiometric amounts of starting materials were mixed and ground well in ethanol with a mortar and pestle, and then the slurries were dried, pelleted and calcined

at 900 °C for 12 h. Subsequently, the pellets were pulverized. The obtained powders were pressed into pellets again and then calcined in air at 1000 °C for 12 h, with heating and cooling rates of 250 °C·h^{-1}.

The microstructures of the samples were investigated by a scanning electron microscope (SEM, S-4700, Hitachi, Tokyo, Japan). The phase compositions of the samples were characterized using an X-ray diffractometer (XRD, X'pert Pro MPD, Amsterdam, Netherlands) equipped with a Cu Kα X-ray source (1.5418 Å).

The obtained pellet with a diameter of 16 mm was polished to 1.0 mm thickness. 20% palladium-80% silver paste with silver wires was coated onto each surface of the pellet as electrodes. Electrochemical impedance spectra were performed using an electrochemical station (CHI660E made in China) over the frequency range from 0.1 Hz to 1 MHz at 400-800 °C. Electrical conductivities were measured as a function of temperature in 25°C intervals. In order to study the oxide ionic conduction under oxygen-containing atmospheres, oxygen concentration cells of SNSA and SNS were fabricated: air, Pd-Ag|SNSA or SNS|Pd-Ag, O_2. The theoretical electromotive forces (EMF_{cal}) of the oxygen concentration cells were calculated as: $EMF_{cal} = \frac{RT}{4F} t_O \ln[p_{O_2\,(A)} / p_{O_2\,(B)}]$ when $t_O = 1$ [30]. Finally, the ampere density-voltage (*I-V*) and ampere density-power density (*I-P*) curves for H_2/O_2 fuel cells using $Sr_{0.6}Na_{0.4}Si_{0.9}Al_{0.1}O_{3-\alpha}$ and $Sr_{0.6}Na_{0.4}SiO_{3-\alpha}$ as electrolytes were tested at 800 °C.

3. RESULTS AND DISCUSSION

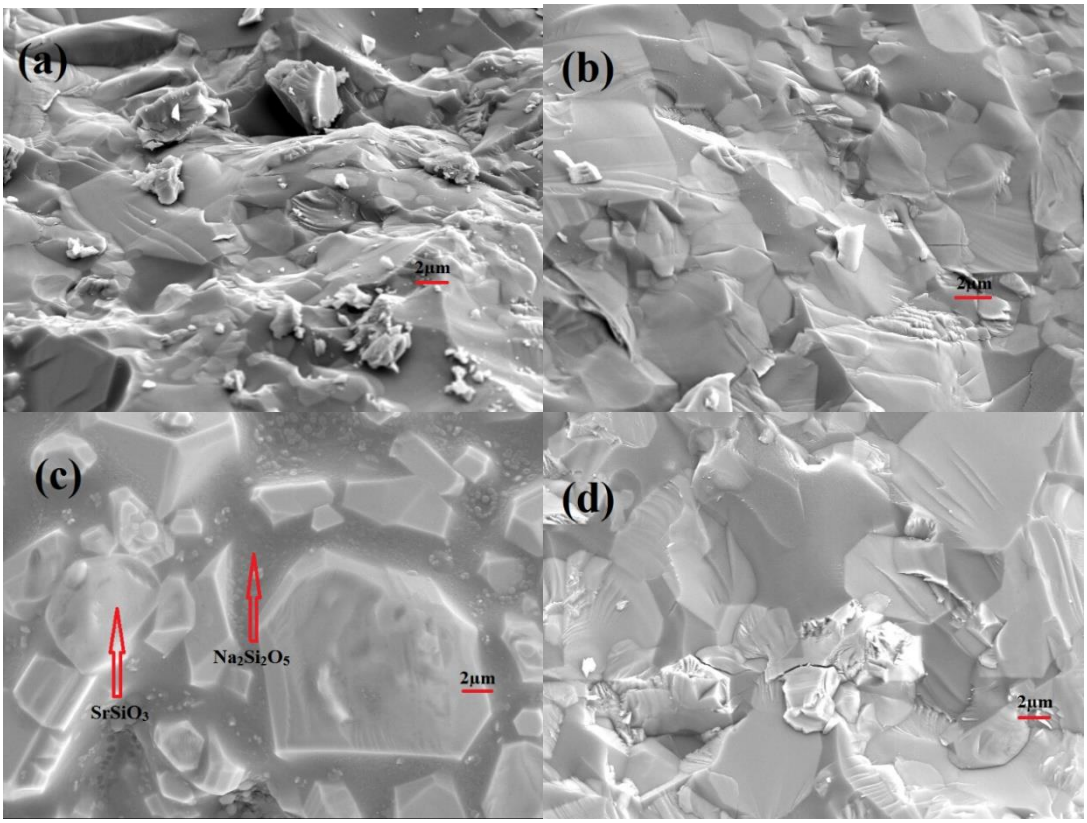

Figure 1. The surface and cross sectional SEM images of the $Sr_{0.6}Na_{0.4}Si_{0.9}Al_{0.1}O_{3-\alpha}$(a,b) and $Sr_{0.6}Na_{0.4}SiO_{3-\alpha}$(c,d) pellets.

Fig.1 shows the surface and cross sectional SEM images of the $Sr_{0.6}Na_{0.4}Si_{0.9}Al_{0.1}O_{3-\alpha}$(a,b) and $Sr_{0.6}Na_{0.4}SiO_{3-\alpha}$(c,d) pellets sintered at 1000 °C for 12 h. It can be observed that both samples are fully-dense and nonporous. Because the synthesis temperature is higher than the melting point of $Na_2Si_2O_5$, two different phases can be clearly seen in Fig.1, which illustrates that both Na-doped samples are composed of two different compositions, amorphous $Na_2Si_2O_5$ and crystalline $SrSiO_3$ [25].

Fig. 2 displays the powder XRD patterns of the $Sr_{0.6}Na_{0.4}Si_{0.9}Al_{0.1}O_{3-\alpha}$ (SNSA) and $Sr_{0.6}Na_{0.4}SiO_{3-\alpha}$ (SNS) samples. It can be seen clearly that the peaks of the two samples are consistent with the standard diffraction pattern of $SrSiO_3$ (PDF No. 87-0474) as reported by Sood et al. [29] and there is no other crystalline phase. Although the amorphous phase could not be detected by XRD, the majority of Na^+ resides in the amorphous $Na_2Si_2O_5$ phase. Moreover, the peak intensities of SNSA are a little stronger than that of SNS in Fig. 2. This may be caused by the minor substitution of Al^{3+} into Si^{4+} in SNSA. This means that the presence of Na^+ and Al^{3+} favors the formation of the $SrSiO_3$ crystalline phase, which in turn may decrease the amount of amorphous phase in this sample.

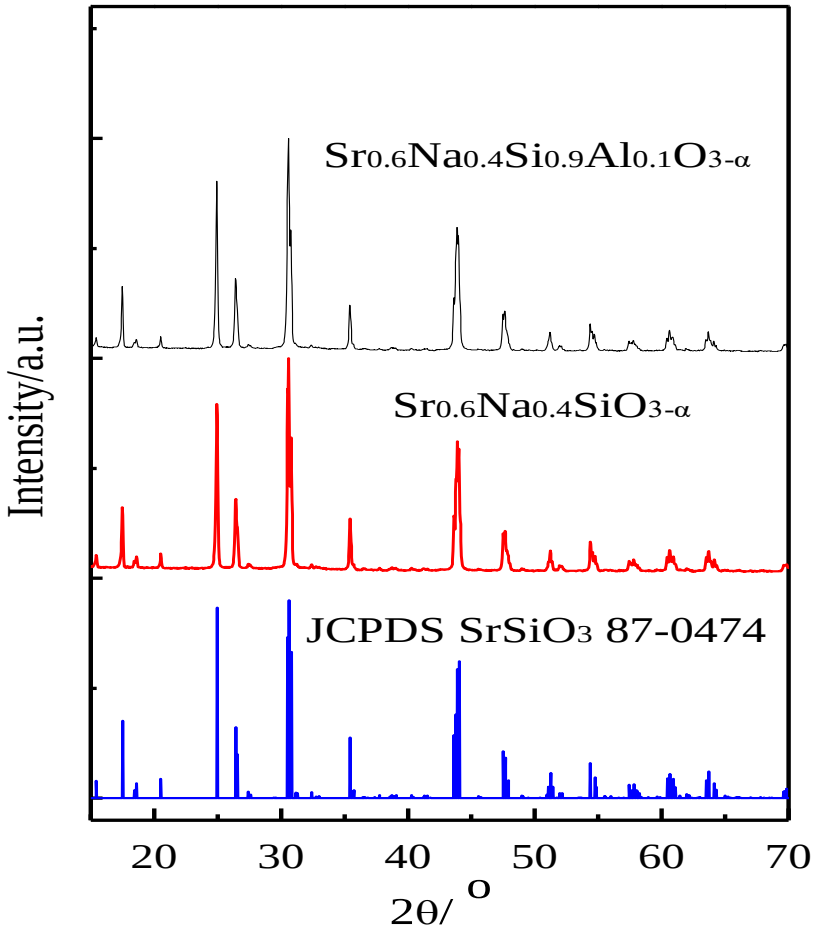

Figure 2. XRD patterns of the $Sr_{0.6}Na_{0.4}Si_{0.9}Al_{0.1}O_{3-\alpha}$ (SNSA) and $Sr_{0.6}Na_{0.4}SiO_{3-\alpha}$ (SNS) samples

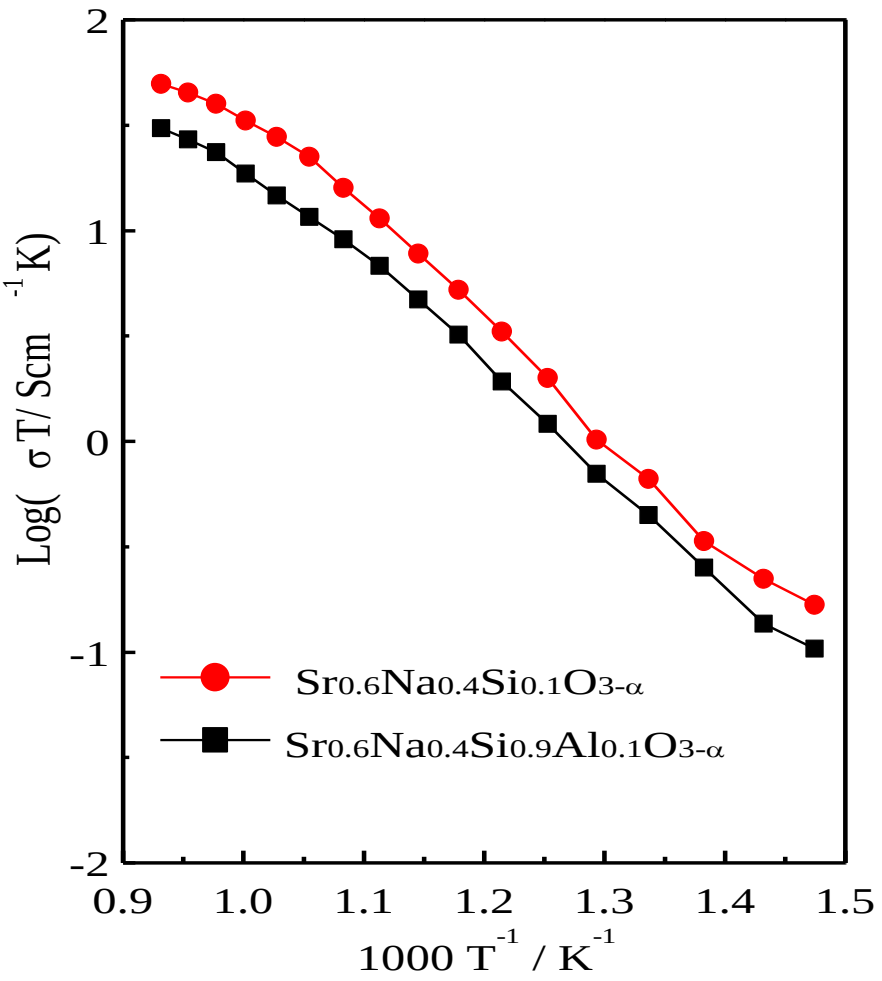

Figure 3. Arrhenius plots of log(σT) vs. 1000/T for $Sr_{0.6}Na_{0.4}Si_{0.9}Al_{0.1}O_{3-\alpha}$ and $Sr_{0.6}Na_{0.4}SiO_{3-\alpha}$

Fig.3 shows the Arrhenius plots of conductivities for $Sr_{0.6}Na_{0.4}Si_{0.9}Al_{0.1}O_{3-\alpha}$ and $Sr_{0.6}Na_{0.4}SiO_{3-\alpha}$ in the temperature range of 400-800 °C in a nitrogen atmosphere. The result shows that the electrical conductivities of both samples increase with increasing temperature and the conductivities of $Sr_{0.6}Na_{0.4}SiO_{3-\alpha}$ are higher than that of $Sr_{0.6}Na_{0.4}Si_{0.9}Al_{0.1}O_{3-\alpha}$ in the whole experimental temperature range. The electrical conductivities reach the highest values of 28.5 $mS \cdot cm^{-1}$ and 46.3 $mS \cdot cm^{-1}$ at 800 °C for $Sr_{0.6}Na_{0.4}Si_{0.9}Al_{0.1}O_{3-\alpha}$ and $Sr_{0.6}Na_{0.4}SiO_{3-\alpha}$, respectively. Our result was less than that reported by Singh and Goodenough [16] ($Sr_{0.6}Na_{0.4}SiO_{3-\alpha}$, σ = 63 $mS \cdot cm^{-1}$ at 700℃), and two times higher than reported by Sood et al. [29] ($Sr_{0.6}Na_{0.4}SiO_{3-\delta}$, σ = 22.8 $mS \cdot cm^{-1}$ at 800 °C in air). The Al^{3+} ion doping in the $Sr_{1-x}Na_xSiO_{3-\alpha}$ system leads to the decrement of the amorphous Na-rich phase and has a negative effect on the conductivity.

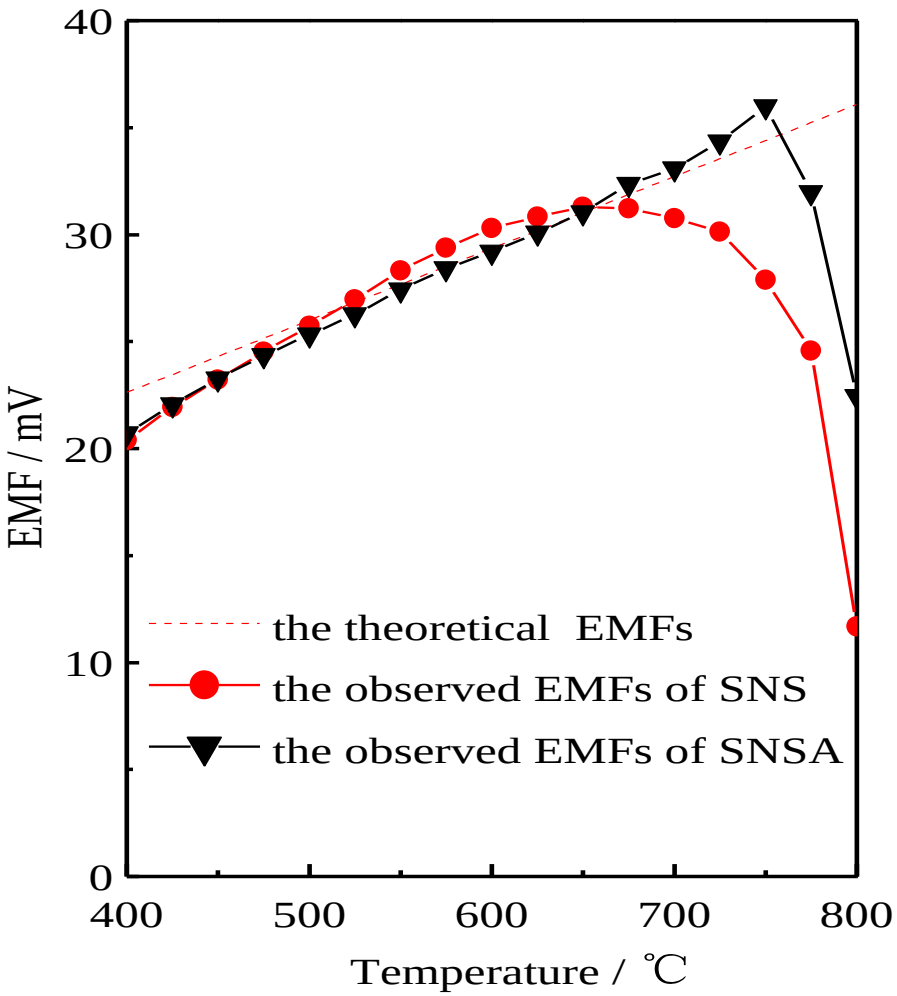

Figure 4. EMFs of oxygen concentration cells of $Sr_{0.6}Na_{0.4}Si_{0.9}Al_{0.1}O_{3-\alpha}$ (SNSA) and $Sr_{0.6}Na_{0.4}SiO_{3-\alpha}$ (SNS) at 400–800 °C.

The theoretical EMFs of oxygen concentration cells and observed EMFs of $Sr_{0.6}Na_{0.4}Si_{0.9}Al_{0.1}O_{3-\alpha}$ (SNSA) and $Sr_{0.6}Na_{0.4}SiO_{3-\alpha}$ (SNS) are shown in Fig. 4. From Fig. 4, the observed EMFs of $Sr_{0.6}Na_{0.4}Si_{0.9}Al_{0.1}O_{3-\alpha}$ (400–750 °C) and $Sr_{0.6}Na_{0.4}SiO_{3-\alpha}$ (400–650 °C) agree well with the theoretical EMFs values. The Al^{3+} ion doping in the $Sr_{0.6}Na_{0.4}SiO_{3-\alpha}$ reduces the content of amorphous $Na_2Si_2O_5$ and extends the scope of the oxide ionic conduction. However, the oxide ion transport numbers sharply decrease near the melting point of amorphous $Na_2Si_2O_5$. The results demonstrate that $Sr_{0.6}Na_{0.4}Si_{0.9}Al_{0.1}O_{3-\alpha}$ (400–750 °C) and $Sr_{0.6}Na_{0.4}SiO_{3-\alpha}$ (400–650 °C) are good oxide ion conductors and mixed conductors of Na^+ and oxide ion at high temperature.

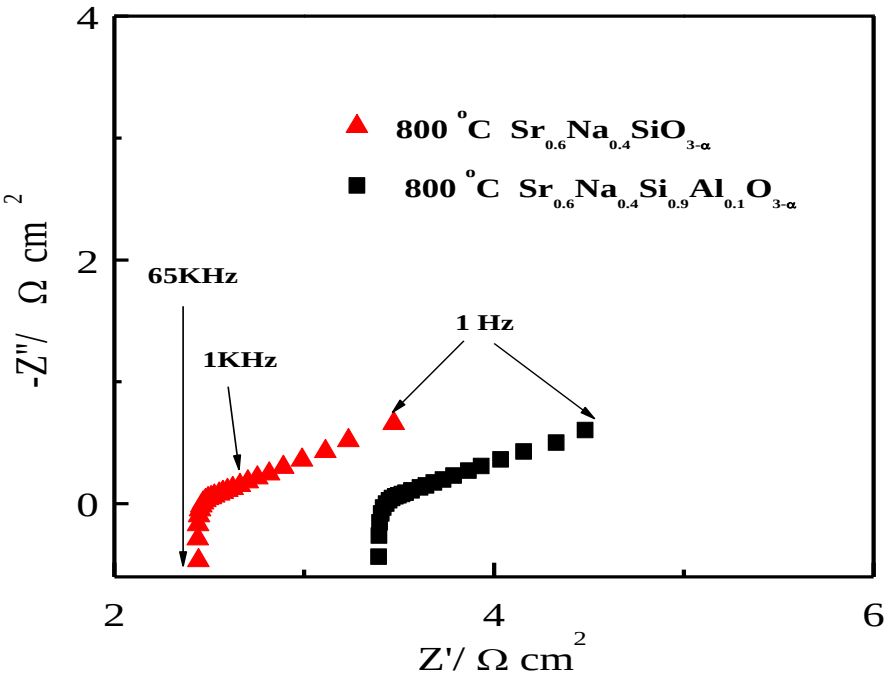

Figure 5. Impedance spectra of $Sr_{0.6}Na_{0.4}Si_{0.9}Al_{0.1}O_{3-\alpha}$ (SNSA) and $Sr_{0.6}Na_{0.4}SiO_{3-\alpha}$ (SNS) under open circuit condition at 800 °C.

Fig. 5 shows the impedance spectra of $Sr_{0.6}Na_{0.4}Si_{0.9}Al_{0.1}O_{3-\alpha}$ and $Sr_{0.6}Na_{0.4}SiO_{3-\alpha}$ under open circuit condition at 800 °C. The impedance spectrum usually consists of two well defined semicircles, the low frequency semicircle corresponds to grain boundary resistance, whereas the high frequency semicircle corresponds to grain contribution [29]. As can be seen from Fig. 5, there are no clear semicircles, and it is difficult to separate the contribution of the grain boundary and the grain. This may be due to the high resistances of the samples. We obtained the total resistance from the intercept of the linear region of the curve to the real axis [27–28]. The resistance of $Sr_{0.6}Na_{0.4}Si_{0.9}Al_{0.1}O_{3-\alpha}$ (3.42 $\Omega \cdot cm^2$) is higher than $Sr_{0.6}Na_{0.4}SiO_{3-\alpha}$ (2.46 $\Omega \cdot cm^2$) under open circuit condition.

Fig. 6 shows the performances of H_2/O_2 fuel cells with $Sr_{0.6}Na_{0.4}Si_{0.9}Al_{0.1}O_{3-\alpha}$ and $Sr_{0.6}Na_{0.4}SiO_{3-\alpha}$ electrolytes at 800 °C. It is observed that the Al dopant strongly influences the performance of the H_2/O_2 fuel cell. Maximum power densities of 39.5 and 79.8 $mW \cdot cm^{-2}$ are achieved at 800 °C in $Sr_{0.6}Na_{0.4}Si_{0.9}Al_{0.1}O_{3-\alpha}$ and $Sr_{0.6}Na_{0.4}SiO_{3-\alpha}$ electrolytes, respectively. The maximum power densities are low which may be due to the samples being Na^+ and oxide ion mixed conductors at 800 °C, as we discussed above. And the Al^{3+} ion doping in the $Sr_{1-x}Na_xSiO_{3-\alpha}$ system has a negative effect on the conductivity, therefore, the maximum power density of $Sr_{0.6}Na_{0.4}Si_{0.9}Al_{0.1}O_{3-\alpha}$ is lower than that of $Sr_{0.6}Na_{0.4}SiO_{3-\alpha}$.

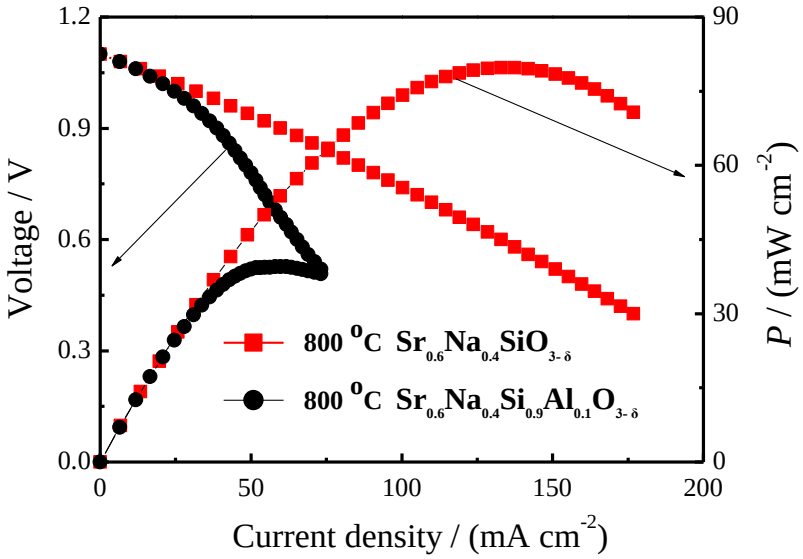

Figure 6. I-V and I-P curves of the H_2/O_2 fuel cells with $Sr_{0.6}Na_{0.4}Si_{0.9}Al_{0.1}O_{3-\alpha}$ and $Sr_{0.6}Na_{0.4}SiO_{3-\alpha}$ electrolyte at 800 °C.

4. CONCLUSIONS

The ionic conductors have important applications in intermediate temperature solid oxide fuel cells (IT-SOFCs). $Sr_{0.6}Na_{0.4}Si_{0.9}Al_{0.1}O_{3-\alpha}$ and $Sr_{0.6}Na_{0.4}SiO_{3-\alpha}$ were successfully fabricated using solid state synthesis method. The results of XRD and SEM demonstrated that both samples consist of crystalline $SrSiO_3$ and amorphous $Na_2Si_2O_5$. Substitution of Si^{4+} by low valence Al^{3+} ion in the $Sr_{1-x}Na_xSiO_{3-\alpha}$ system has a negative effect on the conductivity. The oxygen concentration cells results demonstrate that $Sr_{0.6}Na_{0.4}Si_{0.9}Al_{0.1}O_{3-\alpha}$ (400–750 °C) and $Sr_{0.6}Na_{0.4}SiO_{3-\alpha}$ (400–650 °C) are good oxide ion conductors and mixed conductors of Na^+ and oxide ion at high temperature.

ACKNOWLEDGEMENTS
This work was supported by the National Natural Science Foundation (No. 51402052) of China, The Natural Science Project of Anhui Province (No. KJ2018A0337), Excellent Youth Foundation of Anhui Educational Committee (No. gxyq2018046), Horizontal cooperation project of Fuyang municipal government and Fuyang Normal College (No. XDHX2016019, XDHXTD201704, XDHX201739), Excellent Youth Foundation of Fuyang Normal College (rcxm201805) and Foundation of Anhui Provincial Key Laboratory for Degradation and Monitoring of Pollution of the Environment (2019HJJC01ZD).

References

1. G. L. Liu, W. Liu Q. Kou and S. J. Xiao, *Int. J. Electrochem. Sci.*, 13 (2018) 2641.
2. Y. Yang, H. Hao, L. Zhang, C. Chen, Z. Luo, Z. Liu, Z. Yao, M. Cao and H. Liu, *Ceram. Int.*, 44 (2018) 11109.
3. Y. N. Chen, T. Tian, Z. H. Wan, F. Wu, J. T. Tan and M. Pan, *Int. J. Electrochem. Sci.*, 13 (2018) 3827.

4. T. Hibino, K. Kobayashi, P. Lv, M. Nagao, S. Teranishi, and T. Mori, *J. Electrochem. Soc.*, 164 (2017) F557.
5. S. Lee, and X. Guan, *MRS Communications*, 7 (2017) 199.
6. J. Luo, A.H. Jensen, N.R. Brooks, J. Sniekers, M. Knipper, D. Aili, Q. Li, B. Vanroy, M. Wübbenhorst, F. Yan, L.V. Meervelt, Z. Shao, J. Fang, Z.-H. Luo, D.E.D. Vos, K. Binnemans, and J. Fransaer, *Energy Environ. Sci.*, 8 (2015) 1276.
7. A.A. Solovyev, S.V. Rabotkin, A.V. Shipilova and I.V. Ionov, *Int. J. Electrochem. Sci*., 14 (2019) 575.
8. C. Xia, Z. Qiao, C. Feng, J. Kim, B. Wang and B. Zhu, *Materials*, 11(2018) 40.
9. Y. Tian, Z. Lü, X. Guo and P. Wu, *Int. J. Electrochem. Sci*., 14 (2019) 1093.
10. Z. Zhang, L. Chen, Q. Li, T. Song, J. Su, B. Cai, H. He, *Solid State Ionic*s, 323 (2018) 25.
11. W. Wang, D. Medvedev and Z. Shao, *Adv. Funct. Mater.*, 28 (2018) 1802592.
12. S.H. Morejudo, R. Zanón, S. Escolástico, I. Yuste-Tirados, H. Malerød-Fjeld, P.K. Vestre, W.G. Coors, A. Martínez, T. Norby, J.M. Serra and C. Kjølseth, *Science*, 353 (2016) 563.
13. E. Pikalova and D. Medvedev, *Int. J. Hydrogen Energy,* 41 (2016) 4016.
14. S. Y. Bae, J.-Y. Park and H.-T. Lim, *Electrochim. Acta*, 236 (2017) 399.
15. P. Singh and J.B. Goodenough, *Energy Environ. Sci.*, 5 (2012) 9626.
16. P. Singh and J.B. Goodenough, *J. Am. Ceram. Soc.*, 135 (2013) 10149.
17. T. Wei, P. Singh, Y. Gong, J.B. Goodenough, Y. Huang and K. Huang, *Energy Environ. Sci.*, 7 (2014) 1680.
18. J. Xu, X. Wang, H. Fu, C.M. Brown, X. Jing, F. Liao, F. Lu, X. Li, X. Kuang and M. Wu, *Inorg. Chem.*, 53 (2014) 6962.
19. R.D. Bayliss, S.N. Cook, S. Fearn, J.A. Kilner, C. Greaves and S.J. Skinner, *Energy Environ. Sci.*, 7 (2014) 2999.
20. I.R. Evans, J.S.O. Evans, H.G. Davies, A.R. Haworth and M.L. Tate, *Chem. Mater.*, 26 (2014) 5187.
21. R.D. Bayliss, S.N. Cook, D.O. Scanlon, S. Fearn, J. Cabana, C. Greaves, J.A. Kilner and S.J. Skinner, *J. Mater. Chem. A*, 2 (2014) 17919.
22. J.R. Peet, C.M. Widdifield, D.C. Apperley, P. Hodgkinson, M.R. Johnson and I.R. Evans, *Chem. Commun.*, 51 (2015) 17163.
23. P.-H. Chien, Y. Jee, C. Huang, R. Dervisoglu, I. Hung, Z. Gan, K. Huang and Y.-Y. Hu, *Chem. Sci.*, 7 (2016) 3667.
24. K.K. Inglis, J.P. Corley, P. Florian, J. Cabana, R.D. Bayliss and F. Blanc, *Chem. Mater.*, 28 (2016) 3850.
25. C.Tealdi, L. Malavasi, I. Uda, C. Ferrara, V. Berbenni and P. Mustarelli, *Chem. Commun.*, 50 (2014) 14732.
26. Y. Jee, X. Zhao and K. Huang, *Chem. Commun.*, 51(2015) 9640.
27. Y. Jee, X. Zhao, X. Lei and K. Huang, *J. Am. Ceram. Soc.*, 99 (2016) 324.
28. J. Xu, S. Liu, Q. Wang, J. Xiaofeng, X. Li and X. Kuang, *J. Mater. Chem. A*, 4 (2016) 6313.
29. K. Sood and S. Basu, *RSC Adv.*, 6 (2016) 20211.
30. J. Guan, S.E. Dorris, U. Balachardran and M. Liu, *Solid State Ionics*, 100 (1997) 45.